Consistency and complexity in coupled semiconductor lasers with time-delayed optical feedback

Kazutaka Kanno[*] and Atsushi Uchida[†]

Department of Information and Computer Sciences, Saitama University, 255 Shimo-okubo, Sakura-ku,
Saitama City, Saitama, 338-8570, Japan

Consistency of response in a system driven repeatedly by a complex signal has been observed in many nonlinear dynamical systems. We investigate the consistency of unidirectionally coupled semiconductor lasers with optical feedback and measure the complexity of the entire laser system by using the Lyapunov spectrum. The complexity strongly depends on the degree of consistency. It is found that the complexity of the coupled laser system can be classified into three regions. When the system shows consistency, the complexity of the entire laser system corresponds to that of the solitary drive laser. In the inconsistency region, the complexity of the entire laser system corresponds to the sum of the complexity of the uncoupled drive and response lasers. The complexity increases more than the sum of the two solitary lasers near the boundary of the consistency region, where new dynamical fluctuations appear due to the optical carrier interaction between the two lasers.

I. INTRODUCTION

Many nonlinear dynamical systems have an ability to generate consistent outputs when driven by a repeated external signal, and this phenomenon is referred to as reliability [1–3] or consistency [4–6]. Consistency can be defined as the ability of a dynamical system to produce an identical response output after some transient period, when the system is driven by a repeated drive signal. We consider a situation where a nonlinear dynamical system (called a response system) is driven by a repeated complex signal such as a chaotic or noise signal. The response system may not produce similar temporal outputs because of different initial conditions for different trials of the drive input. However, if the response system has consistency, an identical complex temporal wave form of the response system can be obtained at each repetition of the drive input.

Consistency of response has been experimentally observed in many nonlinear dynamical systems [1–6]. Consistent response subject to a common drive signal has been reported in the context of generalized synchronization [7–11] and common-noise-induced synchronization [12–20]. The concept of consistency could be applied for an implementation of physical one-way function [21], where an output signal can be easily produced from an input signal through a complex function, whereas the input signal cannot be estimated from the output signal. The physical implementation of one-way function has been reported with a token with complex speckle scattering patterns of light [21]. Instead of using spatial complex patterns, temporal dynamics may be useful when a dynamical system has consistent response. The use of consistency may lead to a new technique of the implementation of physical one-way function, which could be a key technique for hardware-oriented information security systems [22].

The concept of consistency can be also applied for information processing. Recently, reservoir computing with a time-delayed nonlinear dynamical system has been proposed

and demonstrated for speech recognition [23,24]. Consistent response output with respect to a drive signal is required for the application of reservoir computing.

One of the important characteristics for the applications of physical one-way function and reservoir computing is the complexity of the functional system. The complexity has been analyzed in many nonlinear dynamical systems with different techniques, such as statistical complexity [25,26], permutation entropy [27–29], nontriviality measure [30], Karhunen-Loève decomposition [31], correlation dimension [32], and Kolmogorov-Sinai (KS) entropy [33,34]. Most techniques are based on statistical measurement of time series analysis using observed data that includes undesirable noise. On the contrary, KS entropy, which is a measure of complexity based on Lyapunov spectrum analysis, could be more reliable since the complexity can be obtained from integration of linearized equations of a numerical model. KS entropy indicates the divergence of tiny errors on a chaotic trajectory in a multidimensional phase space, and it is estimated from the sum of positive Lyapunov exponents. KS entropy is also a measure of unpredictability of the nonlinear dynamical system. Another important measure obtained from Lyapunov spectrum analysis is Kaplan-Yorke (KY) dimension, which indicates the minimum degree of freedom to describe the dynamics of the system. KY dimension can be obtained from a number of Lyapunov exponents as well. Some works on the calculation of KS entropy and KY dimension have been reported in time-delayed nonlinear dynamical systems [33,34].

Semiconductor lasers with time-delayed optical feedback are good candidates for implementing physical one-way function and reservoir computing, which requires high-frequency generation of chaotic complex signals in a consistent way with respect to a complex drive signal. For semiconductor lasers, KS entropy and KY dimension for a single semiconductor laser with time-delayed optical feedback has been reported [34]. However, the complexity of optically coupled semiconductor lasers has not been reported. Moreover, the relationship between consistency and complexity in coupled laser systems has not been investigated yet. It is an important question how the complexity of a coupled nonlinear dynamical system changes when the state of consistency is varied.

---
[*]s11dm001@mail.saitama-u.ac.jp
[†]auchida@mail.saitama-u.ac.jp

In this study we investigate consistency of response in unidirectionally coupled semiconductor lasers with time-delayed optical feedback and measure the complexity of the coupled laser system by using Lyapunov spectrum analysis. We quantitatively evaluate the complexity of the coupled entire laser system by using KS entropy and KY dimension, estimated from Lyapunov exponents. We clarify the conditions how the complexity changes for different states of consistency in the coupled laser system.

II. MODEL FOR NUMERICAL SIMULATIONS

We numerically investigate the conditions to obtain consistency in unidirectionally coupled semiconductor lasers with time-delayed optical feedback. A model consisting of two semiconductor lasers (called drive and response lasers) is shown in Fig. 1. Each laser has an external mirror for generating chaos due to time-delayed optical feedback. The drive signal is injected into the response laser to observe consistency. We repeated numerical simulation twice with the same parameter values but different initial conditions for the response laser that are subject to an identical chaotic temporal wave form from the drive laser. The outputs of the response laser for the two repeated trials are referred to as response 1 and response 2 outputs, respectively. Consistency can be observed when the correlation between the response 1 and 2 outputs is large, even though the correlation between the drive and response is relatively low.

The model shown in Fig. 1 can be described by a set of coupled rate equations for semiconductor lasers, known as the Lang-Kobayashi equations [6,34–36]. The unidirectionally coupled Lang-Kobayashi equations are described as follows.

Drive laser:

$$\frac{dE_d(t)}{dt} = \frac{1 + i\alpha}{2} \left\{ G_N[N_d(t) - N_0] - \frac{1}{\tau_p} \right\} E_d(t) + \kappa_d E_d(t - \tau_d) \exp(-i\omega_d \tau_d) \quad (1)$$

$$\frac{dN_d(t)}{dt} = J_d - \frac{N_d(t)}{\tau_s} - G_N[N_d(t) - N_0]|E_d(t)|^2 \quad (2)$$

Response laser:

$$\frac{dE_r(t)}{dt} = \frac{1 + i\alpha}{2} \left\{ G_N[N_r(t) - N_0] - \frac{1}{\tau_p} \right\} E_r(t) + \kappa_r E_r(t - \tau_r) \exp\{-i(\omega_d - \Delta\omega)\tau_r\} + \kappa_{\text{inj}} E_d(t - \tau_{\text{inj}}) \exp\{i(\Delta\omega t - \omega_d \tau_{\text{inj}})\} \quad (3)$$

$$\frac{dN_r(t)}{dt} = J_r - \frac{N_r(t)}{\tau_s} - G_N[N_r(t) - N_0]|E_r(t)|^2, \quad (4)$$

where E is the complex electric field (a complex variable) and N is the carrier density (a real variable). The subscripts d and r represent the drive and response lasers, respectively.
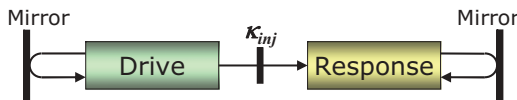

FIG. 1. (Color online) Model for unidirectionally coupled two semiconductor lasers with optical feedback. κ_{inj}: injection strength from the drive to response lasers.

G_N is the gain coefficient, α is the line-width enhancement factor, N_0 is the carrier density at transparency, τ_s is the carrier lifetime, τ_p is the photon lifetime, $\tau_{d,r} = 2L_{d,r}/c$ is the round-trip delay time in the external cavity for the drive and response lasers, and $\tau_{\text{inj}} = L_{\text{inj}}/c$ is the propagation time of the injection light from the drive to response lasers. The feedback coefficient κ_d and κ_r are given by $\kappa_d = (1 - r_2^2)r_{3,d}/(r_2 \tau_{in})$ and $\kappa_r = (1 - r_2^2)r_{3,r}/(r_2 \tau_{in})$, where τ_{in} is the round-trip time in the internal laser cavity. r_2, $r_{3,d}$, and $r_{3,r}$ represent intensity reflectivities of the laser facet and the external mirrors for the drive and response lasers. $\omega_d = 2\pi c/\lambda_d$ and $\omega_r = 2\pi c/\lambda_r$ are the angular optical frequency of the solitary drive and response lasers, where λ_d and λ_r are the optical wavelengths of the solitary drive and response lasers. The injection strength from the drive to response lasers is given by the injection coefficient κ_{inj}. $\Delta\omega = \omega_d - \omega_r$ is the initial optical angular-frequency detuning between the solitary (uncoupled) drive and response lasers, and $\Delta f = \Delta\omega/2\pi$ represents the initial optical-frequency detuning between the solitary drive and response lasers.

The complex variable E is transformed to real and imaginary parts (i.e., $E = E_R + iE_I$) for the convenience of numerical calculations to avoid divergence of integration for small E [6]. We numerically solve the real and imaginary equations by using the fourth-order Runge-Kutta method. The parameter values used in the numerical simulations are shown in Table I. We set the different parameter values for the reflectivities and the injection current between the drive and response lasers (i.e., $r_{3,d} = 0.015$, $r_{3,r} = 0.03$) (These reflectivities result in the feedback strengths of $\kappa_d = 2.33$ ns^{-1} and $\kappa_r = 4.66$ ns^{-1}.), $J_d/J_{\text{th}} = 1.11$, and $J_r/J_{\text{th}} = 1.36$. We used much larger injection strength $\kappa_{\text{inj}} = 31.1$ ns^{-1} than the feedback strengths, because large optical injection is necessary to achieve injection locking of the optical carrier frequencies between the drive and response lasers. The initial optical-frequency detuning is also introduced (i.e., $\Delta f = -4.0$ GHz). The other parameter values are set to be identical between the drive and response lasers, as shown in Table I.

III. CONSISTENCY IN COUPLED SEMICONDUCTOR LASERS

Figures 2(a) and 2(b) show the temporal waveforms of the drive, response 1, and response 2 outputs and the corresponding correlation plot between the response 1 and 2 outputs without optical injection from the drive laser ($\kappa_{\text{inj}} = 0.0$ ns^{-1}). It is found that the outputs of the response 1 and 2 show different temporal behaviors, and the response laser does not show consistency. Next the output of the drive laser is injected into the response laser. Figures 2(c) and 2(d) show the temporal wave forms of the drive, response 1, and response 2 outputs and the corresponding correlation plot between the response 1 and 2 outputs at the injection strength of $\kappa_{\text{inj}} = 31.1$ ns^{-1}. Note that the temporal waveform of the drive output is time-shifted by the propagation time τ_{inj} in Figs. 2(a) and 2(c). The temporal wave forms of the response 1 and 2 are identical, even though they differ from the temporal wave form of the drive laser, as shown in Fig. 2(c). The correlation plot shown in Fig. 2(d) is a straight line at 45 degree, indicating the achievement of consistency of the response laser.

TABLE I. Parameter values used in numerical simulations.

Symbol	Parameter	Value
G_N	Gain coefficient	8.40×10^{-13} m^{3}s^{-1}
N_0	Carrier density at transparency	1.40×10^{24} m^{-3}
τ_p	Photon lifetime	1.927×10^{-12} s
τ_s	Carrier lifetime	2.04×10^{-9} s
τ_{in}	Round-trip time in internal cavity	8.0×10^{-12} s
r_2	Reflectivity of laser facet	0.556
α	Line-width enhancement factor	3.0
λ_d	Optical wavelength of the drive laser	1.55×10^{-6} m
c	Speed of light	2.998×10^{8} ms^{-1}
N_{th}	Carrier density at threshold	2.018×10^{24} m^{-3}
J_{th}	Injection current at threshold	9.892×10^{32} m^{-3}s^{-1}
ω_d	Optical angular frequency of the drive laser	1.215×10^{15} s^{-1}
$r_{3,d}$	Reflectivity of external mirror of drive laser	0.015
$r_{3,r}$	Reflectivity of external mirror of response laser	0.03
κ_d	Feedback strength of drive laser	2.33×10^{-9}s^{-1}
κ_r	Feedback strength of response laser	4.66×10^{-9}s^{-1}
κ_{inj}	Injection strength from the drive to response lasers	3.11×10^{-8}s^{-1}
J_d/J_{th}	Normalized injection current of the drive laser	1.11
J_r/J_{th}	Normalized injection current of the response laser	1.36
$L_{d,r}$	External cavity length of the drive laser (one-way)	0.6 m
L_{inj}	Distance from the drive to response lasers	1.2 m
$\tau_{d,r}$	Round-trip time of light in external cavity (feedback delay time) for the drive or response laser	4.003×10^{-9} s
τ_{inj}	Propagation time of light from the drive to response lasers	4.003×10^{-9} s
Δf	Initial optical-frequency detuning between the drive and response lasers	-4.0×10^{9}Hz
$\Delta\omega$	Initial optical-angular frequency detuning between the drive and response lasers	-2.513×10^{10} s^{-1}

It is found that the temporal wave forms of the time-delayed drive and the response lasers are weakly correlated since some peaks appear simultaneously. Phase synchronization may be observed between the drive and response wave forms [8]. These weakly correlated wave forms result from strong optical
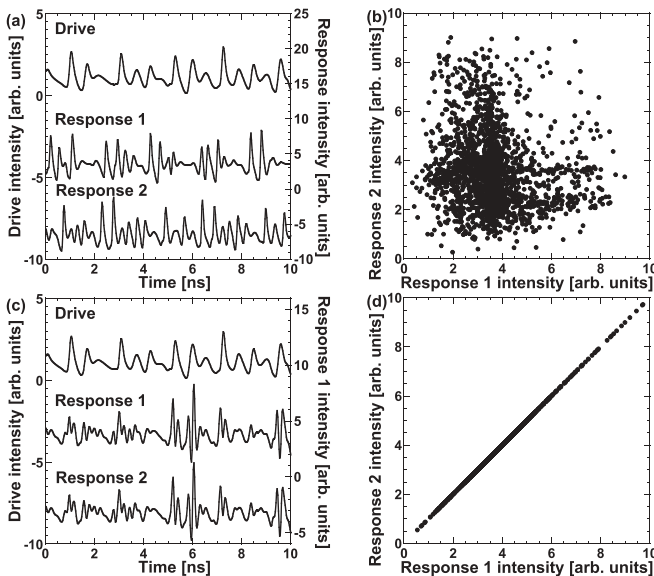

FIG. 2. (a), (c) Temporal wave forms of the time-delayed drive, response 1, and response 2 outputs, and (b), (d) correlation plots between the response 1 and 2 outputs. The injection strengths are (a), (b) $\kappa_{inj} = 0.0$, and (c), (d) $\kappa_{inj} = 31.1$ ns^{-1}.

injection, and may not be desirable for the applications to physical one-way function [21] because it may be easy to predict the response signal only from the drive signal. A constant-amplitude and random-phase (CARP) signal [37] could be used as a drive signal for this type of application, instead of a chaotic drive signal, to avoid the correlation between the drive and response wave forms.

We quantitatively evaluate the degree of consistency by using the cross correlation between the response 1 and 2 outputs as follows,

$$C_{r1,r2} = \frac{\langle [I_{r1}(t) - \bar{I}_{r1}][I_{r2}(t) - \bar{I}_{r2}] \rangle}{\sigma_{r1}\sigma_{r2}}, \quad (5)$$

where $I(t)$ is the intensity of the response laser, $\bar{I}$ is the mean value of the laser intensity, σ is the standard deviation of the laser intensity, and $<>$ is the time averaging. The subscripts $r1$ and $r2$ represent the response 1 and 2 outputs, respectively. We also calculated the cross correlation between the time-delayed drive and response 1 outputs as,

$$C_{d,r1} = \frac{\langle [I_d(t - \tau_{inj}) - \bar{I}_d][I_{r1}(t) - \bar{I}_{r1}] \rangle}{\sigma_d\sigma_{r1}}, \quad (6)$$

where the subscripts d and $r1$ represent the drive and response 1 outputs, respectively.

In optically coupled semiconductor lasers, injection locking is crucial for chaos synchronization, where the optical frequency of the response laser is matched to that of the drive laser [6]. An important question arises whether injection locking occurs when consistency is achieved. We thus calculated the optical frequency detuning with optical injection from the drive
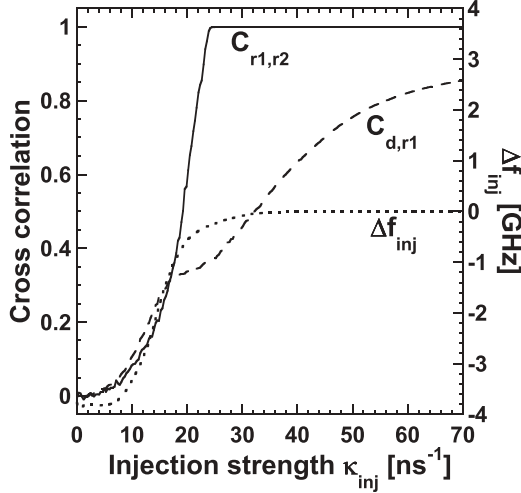
FIG. 3. Cross correlations between the response 1 and 2 outputs $C_{r1,r2}$ (solid curve) and between the time-delayed drive and response 1 outputs $C_{d,r1}$ (dashed curve) as a function of the injection strength κ_{inj}. The optical frequency detuning with optical injection Δf_{inj} (dotted curve) is also plotted.

to response lasers Δf_{inj} [6,38].

$$\Delta f_{\mathrm{inj}} = \Delta f + \frac{1}{2\pi} \left[\frac{d\phi_d(t)}{dt} - \frac{d\phi_r(t)}{dt} \right], \qquad (7)$$

where $\phi_d(t)$ and $\phi_r(t)$ are the phase of electric field for the drive and response lasers, and calculated from $\phi(t) = \tan^{-1}[E_I(t)/E_R(t)]$. Δf is the initial optical-frequency detuning between the drive and response lasers without optical injection. Even for $\Delta f \neq 0$, the optical frequency detuning Δf_{inj} can be close to zero with optical injection by injection locking.

The cross correlation $C_{r1,r2}$ and $C_{d,r1}$ are plotted as a function of the injection strength κ_{inj}, as shown in Fig. 3. The solid and dashed curves represent $C_{r1,r2}$, and $C_{d,r1}$ respectively. In the region of $\kappa_{\mathrm{inj}} > 24.0\mathrm{ns}^{-1}$, $C_{r1,r2}$ is close to 1, indicating consistency. Within this region, $C_{d,r1}$ is changed from 0.4 to 0.8, indicating that the response output differs from the drive output.

The optical frequency detuning Δf_{inj} with optical injection is also plotted as the dotted curve in Fig. 3. Without optical injection ($\kappa_{\mathrm{inj}} = 0\mathrm{ns}^{-1}$), Δf_{inj} is close to the initial optical-frequency detuning $\Delta f = -4.0$ GHz. As κ_{inj} is increased, Δf_{inj} changes and becomes $|\Delta f_{\mathrm{inj}}| < 0.1$ GHz at $\kappa_{\mathrm{inj}} > 29.5\mathrm{ns}^{-1}$. When κ_{inj} is increased further, Δf_{inj} converges to ~ 0 GHz, indicating injection locking. Compared Δf_{inj} with $C_{r1,r2}$ (the solid curve), consistency is observed ($C_{r1,r2} \approx 1.0$) when injection locking is achieved ($\Delta f_{\mathrm{inj}} \approx 0$ GHz). Therefore, consistency is achieved under the condition of injection locking.

IV. LYAPUNOV SPECTRUM ANALYSIS

A. Entropy and dimensionality

To obtain the complexity of the coupled laser system, we calculated KS entropy and KY dimension, which can be estimated from Lyapunov exponents. We derived linearized equations for small deviations from the original trajectory

obtained from the original rate equations of Eqs. (1)–(4) [6]. We numerically solved the linearized equations, and calculated a norm of the linearized variables. For time-delayed nonlinear dynamical systems, all the linearized variables that are included in the delay time need to be regarded as independent variables for the calculation of the norm [6,33,34,39]. The maximum Lyapunov exponent can be calculated from the time average of the logarithm of the norm.

For multidimensional nonlinear dynamical systems, a number of Lyapunov exponents exist, which are called the Lyapunov spectrum. For time-delayed systems, many Lyapunov exponents exist due to the time-delay effect. It is necessary to use a number of sets of the linearized equations to calculate the Lyapunov spectrum for time-delayed dynamical systems, where the number of the sets of the equations corresponds to the number of the Lyapunov exponents obtained in the calculation. The linearized variables can be regarded as components of norm vectors, and orthogonalization is applied to the norm vectors [6,34]. Lyapunov spectrum can be obtained by calculating the time average of logarithm of the norm of the orthogonal vectors.

KS entropy h_{KS} can be calculated from the sum of positive Lyapunov exponents [6,34],

$$h_{\mathrm{KS}} = \sum_{i|\lambda>0} \lambda_i. \qquad (8)$$

KS entropy indicates a loss rate of information. A large value of KS entropy indicates that the system has large unpredictability.

KY dimension D_{KY} (also known as Lyapunov dimension) can be calculated as follows [6,34],

$$D_{\mathrm{KY}} = j + \frac{\sum_{i=1}^{j} \lambda_i}{|\lambda_{j+1}|}, \qquad (9)$$

where j satisfies the following relationship:

$$\sum_{i=1}^{j} \lambda_i > 0 > \sum_{i=1}^{j+1} \lambda_i, \qquad (10)$$

where $\lambda_i > \lambda_k$ $(i < k)$ is satisfied. KY dimension indicates the number of variables to represent dynamical systems. A large number of KY dimension corresponds to more complex dynamics of the systems.

B. Dependence of complexity on injection strength

We measured KS entropy and KY dimension for the coupled entire laser system (both the drive and response lasers), where six variables with time delay exist. For comparison, we also measured KS entropy and KY dimension for the solitary (uncoupled) drive or response laser system. Figure 4 shows KS entropy (solid curve) and KY dimension (dashed curve) of the entire laser system as a function of the injection strength κ_{inj}. The cross-correlation curves of Fig. 3 can be compared with Fig. 4. For the solid curve in Fig. 4, KS entropy is 2.03 ns^{-1} without optical injection ($\kappa_{\mathrm{inj}} = 0$ ns^{-1}). This value equals the sum of the KS entropy for the solitary drive and response lasers without coupling. With increase of κ_{inj}, KS entropy increases and becomes maximum (3.43 ns^{-1}) at $\kappa_{\mathrm{inj}} = 10.6$ ns^{-1}. For larger κ_{inj}, KS entropy decreases and saturates when consistency is achieved in the region of
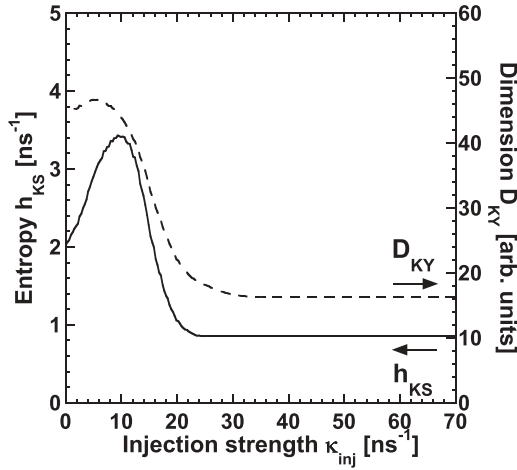
FIG. 4. KS entropy h_{KS} (solid curve) and KY dimension D_{KY} (dashed curve) as a function of the injection strength κ_{inj}.

$\kappa_{inj} > 26.1$ ns^{-1}. The value of KS entropy in the consistency region is 0.85 ns^{-1}, which corresponds to that of the solitary drive laser. Therefore, the complexity of the entire laser system under consistency becomes the minimum value.

For the dashed curve of Fig. 4, KY dimension is obtained as $D_{KY} = 44.1$ without coupling and equals to the sum of KY dimension for the solitary drive and response lasers without coupling, as in the case of KS entropy. However, unlike KS entropy, only a slight increase of KY dimension is observed ($D_{KY} = 46.7$ at maximum) as κ_{inj} is increased. In the consistency region, KY dimension becomes the minimum value ($D_{KY} = 16.3$), which equals that of the solitary drive laser.

To interpret these results, we made comparison among the Lyapunov spectra for the entire laser system, the solitary drive laser, and the solitary response laser. Figure 5(a) shows the Lyapunov spectrum for the entire laser system when the injection strength κ_{inj} is varied. For comparison, Figs. 5(b) and 5(c) show Lyapunov spectra for the solitary drive laser and the solitary response laser, respectively. It is found that the overlap of Figs. 5(b) and 5(c) corresponds to Fig. 5(a). All the Lyapunov exponents for the drive laser [Fig. 5(b)] are constant because the unidirectional injection strength from the drive to response lasers is changed. For the solitary response laser [Fig. 5(c)], all the Lyapunov exponents becomes negative when consistency is achieved. This phenomenon is interpreted that the dynamics of the response laser is totally governed by the drive signal, even though different temporal waveforms of the drive and response lasers are observed. The complexity of the entire laser system is thus dominated by that of the solitary drive laser under consistency ($\kappa_{inj} > 26.1$ ns^{-1}), as shown in Figs. 5(a) and 5(b). Therefore, KS entropy and KY dimension of the entire laser system under consistency is equivalent to that of the solitary drive laser.

C. Dependence of complexity on initial optical-frequency detuning

Next we investigate the relationship between consistency and complexity when the initial optical-frequency detuning is varied between the drive and response lasers. Figure 6(a) shows
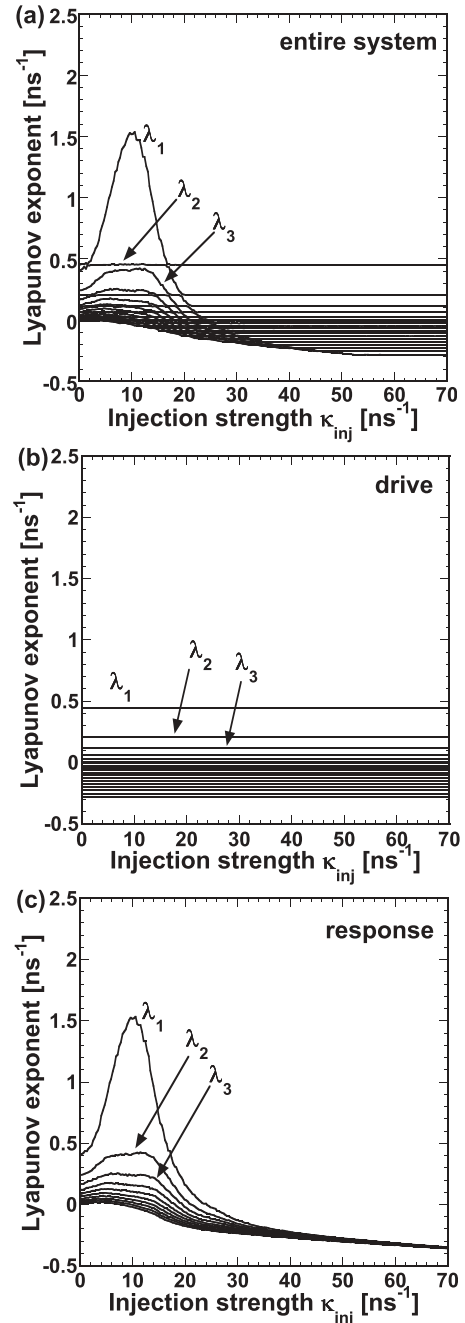

FIG. 5. Lyapunov spectra for (a) the entire laser system (both drive and response), (b) the solitary drive system, and (c) the solitary response system as a function of the injection strength κ_{inj}. 20 largest Lyapunov exponents are shown.

the cross correlation between the response 1 and 2 outputs and between the drive and response 1 outputs as a function of the initial optical-frequency detuning Δf at the fixed injection strength $\kappa_{inj} = 31.1$ ns^{-1}. It is found that consistency is achieved within the range of -6.0 GHz $< \Delta f < 0.0$ GHz as shown in the solid curve of Fig. 6(a). In this region, Δf_{inj} is almost zero and injection locking is achieved. The optical frequency detuning plays an important role for the achievement of consistency.
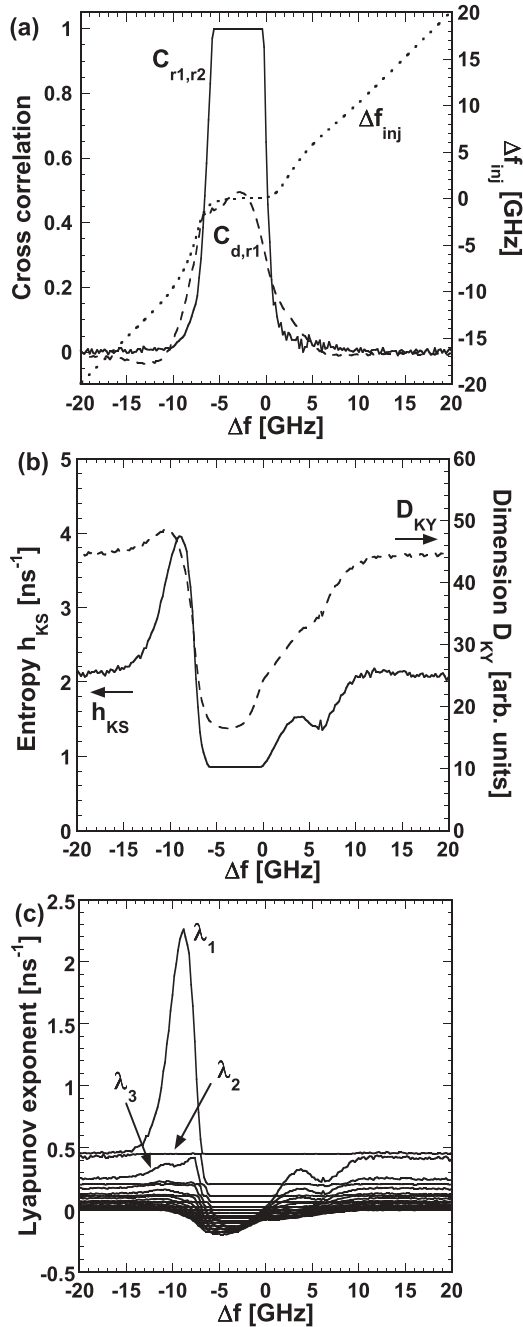
FIG. 6. (a) Cross correlation between the response 1 and 2 outputs $C_{r1,r2}$ (solid curve), between the drive and response 1 outputs $C_{d,r1}$ (dashed curve), and the optical frequency detuning with injection Δf_{inj} (dotted curve), (b) KS entropy h_{KS} (solid curve) and KY dimension D_{KY} (dashed curve), and (c) Lyapunov spectrum λ_i, as a function the initial optical-frequency detuning Δf.

Figure 6(b) shows KS entropy and KY dimension estimated from the Lyapunov spectrum. KS entropy has the largest value at $\Delta f \approx -9$ GHz. From the result of KS entropy shown in Fig. 6(b), the regions of the complexity can be categorized into three regions. First, KS entropy has the lowest value in the region of -6.0 GHz $< \Delta f < 0.0$ GHz, and almost equals to that of the drive laser, where consistency is achieved. Secondly, for large absolute values of the initial optical frequency

detuning ($\Delta f < -15.0$ GHz or $\Delta f > 10.0$ GHz), KS entropy equals to the sum of that of the solitary drive and response lasers. In the third region at $\Delta f \approx -9$ GHz, KS entropy increases, whose value is larger than the sum of the solitary drive and response lasers, at negative detunings outside the consistency region. These characteristics can be seen for KY dimension, although no significant increase of KY dimension is found for negative detunings.

Figure 6(c) shows the Lyapunov spectrum of the entire laser system for different initial optical-frequency detunings. The maximum Lyapunov exponent λ_1 increases when the initial optical-frequency detuning is set to be a negative value in the region of -15.0 GHz $< \Delta f < -6.0$ GHz. In other region, the maximum Lyapunov exponent is almost constant. The Lyapunov spectrum of Fig. 6(c) consists of the Lyapunov exponents for the solitary drive and response lasers. All the Lyapunov exponents corresponding to the response laser are negative in the region of -6.0 GHz $< \Delta f < 0.0$ GHz under the condition of consistency.

V. TWO-DIMENSIONAL MAP OF CONSISTENCY AND COMPLEXITY

Next we systematically investigate the relationship between consistency and complexity when the injection strength κ_{inj} and the initial optical-frequency detuning Δf are changed simultaneously. Figure 7(a) shows the two-dimensional map of the cross-correlation value $C_{r1,r2}$ as functions of κ_{inj} and Δf. The degree of consistency is represented by using grayscale, and the black region corresponds to high consistency ($C_{r1,r2} \approx 1$). It is found that consistency is obtained in the region of large injection strengths κ_{inj} and slightly negative detunings Δf. Figure 7(b) shows the optical frequency detuning Δf_{inj} with optical injection as functions of κ_{inj} and Δf. The consistency region in Fig. 7(a) corresponds to the injection locking range, indicated as the black region in Fig. 7(b), where the optical wavelengths are almost matched between the drive and response lasers by optical injection ($\Delta f_{inj} < 0.1$ GHz).

Figure 8(a) shows the two-dimensional map of KS entropy h_{KS} for the entire laser system as functions of κ_{inj} and Δf. Black regions correspond to large KS entropy. It is found that the complexity of the entire system can be classified into three regions. First, KS entropy becomes low [the white region in Fig. 8(a)], which corresponds to the consistency region [the black region of Fig. 7(a)]. It is worth noting that KS entropy in this region corresponds to KS entropy of the solitary drive laser ($h_{KS} = 0.86$ ns^{-1}). Secondly, when the response laser does not show consistency outside the injection locking range, KS entropy becomes larger [the gray region of Fig. 8(a)]. KS entropy in this region corresponds to the sum of KS entropy of the solitary drive and response lasers ($h_{KS} = 2.03$ ns^{-1}). For the third region, KS entropy becomes the maximum value in the region near the boundary of the consistency region [the black region of Fig. 8(a)]. The maximum value of KS entropy is $h_{KS} = 4.37$ ns^{-1}, which is roughly twice larger than the sum of KS entropy of the solitary drive and response lasers. The region of large KS entropy appears near the boundary of the injection locking range. The asymmetry of the regions for large KS entropy in terms of Δf results
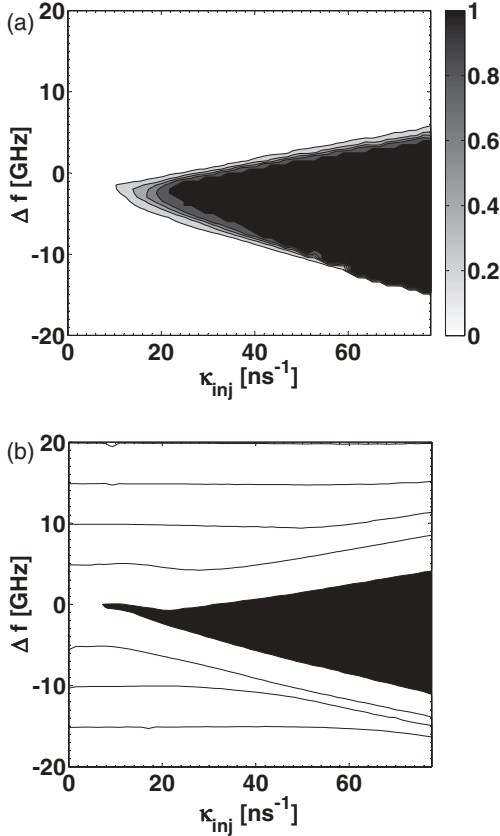
FIG. 7. Two-dimensional maps of (a) the cross correlation $C_{r1,r2}$ between the response 1 and 2 outputs and (b) the optical frequency detuning with optical injection Δf_{inj} as functions of the injection strength κ_{inj} and the initial optical-frequency detuning Δf. (a) Black region corresponds to high consistency. (b) Black region corresponds to the injection locking range ($\Delta f_{\text{inj}} < 0.1$ GHz).
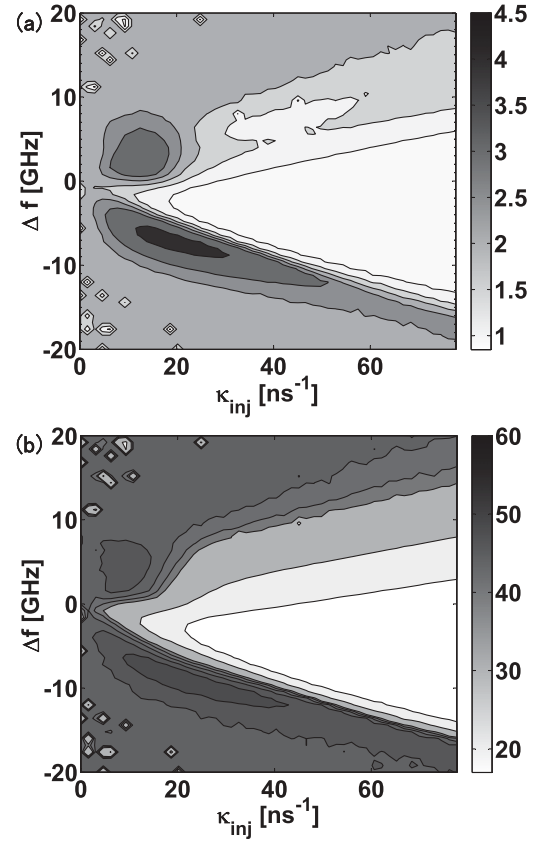

FIG. 8. Two-dimensional maps of (a) KS entropy h_{KS} and (b) KY dimension D_{KY} of the entire laser system as functions of the injection strength κ_{inj} and the initial optical-frequency detuning Δf.

from the line-width enhancement factor α in semiconductor lasers [6,36].

Figure 8(b) shows the two-dimensional map of KY dimension D_{KY} for the entire laser system as functions of κ_{inj} and Δf. Small KY dimension is obtained in the white region of Fig. 8(b), corresponding to the consistency region [the black region of Fig. 7(a)]. In this region, KY dimension corresponds to that for the solitary drive laser ($D_{\text{KY}} = 16.3$). In the inconsistency region, KY dimension becomes larger [the dark gray region of Fig. 8(b)], and KY dimension corresponds to the sum of KY dimension for the solitary drive and response lasers ($D_{\text{KY}} = 44.0$). However, unlike KS entropy of Fig. 8(a), KY dimension is increased slightly in the boundary of the consistency region ($D_{\text{KY}} = 49.2$).

To clarify the mechanism of the entropy enhancement in Fig. 8(a), we investigate the temporal dynamics of the response laser subject to constant optical injection from a stable drive laser. In this situation, both of the drive and response lasers do not have optical feedback, and they are unidirectionally coupled to each other. Figure 9 shows the two-dimensional map of the dynamics of the response laser when κ_{inj} and Δf are changed simultaneously. Stable laser output is observed in the injection locking range, indicated by "S" in Fig. 9. A period-1

(P1) oscillation can be observed in wide regions outside the injection locking range. The frequency of this periodic oscillation roughly corresponds to the initial optical-frequency detuning Δf between the solitary drive and response lasers. Higher-order periodic oscillations and chaotic oscillations occur near the boundary of the injection locking range, indicated by "P2" and "C" in Fig. 9. This complex dynamics has been reported in unidirectionally coupled semiconductor lasers without optical feedback [40–42] and it is considered that the complex dynamics result from the nonlinear interaction between the two optical-carrier frequencies. These parameter regions of P2 and C correspond to the regions where high KS entropy can be obtained in Fig. 8(a). It is worth noting that nonlinear frequency mixing between the two optical-carrier frequencies is responsible for the increase of the complexity in the coupled semiconductor lasers. This phenomenon is unique characteristics for coupled lasers that carry two dominant frequency dynamics (i.e., fast optical-carrier oscillation and slow chaotic envelope oscillation [6]). This significant increase of the complexity by unidirectional coupling has not been observed in other nonlinear dynamical systems such as the Rössler model and the Mackey-Glass model with time-delayed feedback [43].
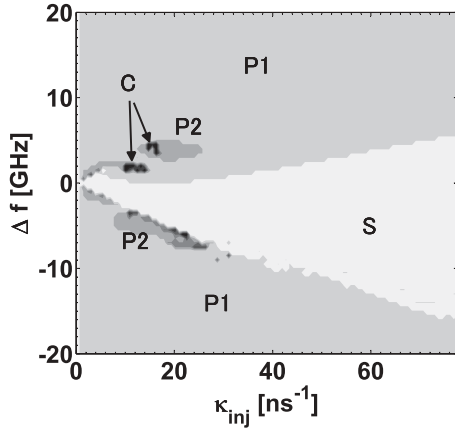
FIG. 9. Two-dimensional map of temporal dynamics for the response laser with optical injection from the stable drive laser as functions of the injection strength κ_{inj} and the initial optical frequency detuning Δf. Both the drive and response lasers do not have optical feedback. S: stable (white region), P1: period-1 oscillation (gray region), P2: period-2 or high-periodic oscillation (dark gray region), C: chaotic oscillation (black region).

VI. DISCUSSION

In this study we quantitatively evaluated the complexity of unidirectionally coupled semiconductor lasers by using the measures of KS entropy and KY dimension based on Lyapunov spectrum analysis, when the state of consistency is varied. We found that the complexity strongly depends on the degree of consistency. The complexity of the entire laser system corresponds to that of the solitary drive laser when the system shows consistency. On the contrary, the complexity of the entire system corresponds to the sum of the complexity of the uncoupled drive and response lasers in the case of inconsistency. More interestingly, the complexity increases more than the sum of the two solitary lasers near the boundary of the consistency region. This third region where the complexity becomes maximum is considered as a unique characteristic of coupled laser systems and has not been observed in other nonlinear dynamical systems [43]. The increase of complexity results from optical-carrier interaction between the drive and response lasers outside the injection locking range, which generates new temporal dynamics as shown in Fig. 9. The lasers have fast optical-carrier components at frequencies of hundreds of THz and the detuning of the optical-carrier frequencies between the two coupled lasers induces complex nonlinear dynamics and increases complexity of the system when the optical frequency locking is incomplete. On the contrary, the two optical frequencies are locked to each other when the strong injection is used and the complexity is governed by the solitary drive laser in the consistency region. This technique for increasing complexity could be used for a physical entropy source in fast physical random number generation [44]. In addition, these findings could be useful for the evaluation of complexity in coupled laser systems for the applications to physical one-way function and reservoir computing [21–24].

The concept of consistency is related to generalized synchronization [7–11]. Generalized synchronization is defined as a functional relationship between the drive and response

temporal wave forms, whereas consistency is defined as reproducibility of a nonlinear dynamical system driven by a repeated complex signal. Generalized synchronization is considered for coupled dynamical systems, however, consistency can be applied for a solitary system. Generalized synchronization can be achieved when all the Lyapunov exponents of the response system become negative. Therefore, it may be expected to show low complexity of the entire system under the achievement of generalized synchronization. This speculation is consistent with our numerical results for complexity and consistency.

The results on ensemble averages of modulated dynamical system have been reported [45,46]. The modulation changes the stability of the dynamical system and this phenomenon is similar to consistency. However, the periodic modulation signal is simpler than the external drive signal from the chaotic drive laser and may result in lower complexity. The analysis of complexity in modulated dynamical systems will be a very interesting topic. In addition, the behavior of a neuronal network driven by a common random drive signal shows both consistency and synchronization [3]. The complexity analysis proposed in this study will be very useful to distinguish between consistency and synchronization in network dynamical systems.

It is required to achieve large complexity and consistency for the applications to physical one-way function [21]. From our results, the complexity becomes the lowest value when the consistency is achieved, and the complexity of the response laser under consistency is determined by that of the solitary drive laser. Therefore, it is important to increase the complexity of the solitary drive laser, but not the response laser, for enhancing the complexity of the physical one-way function implemented by unidirectionally coupled semiconductor lasers.

Coupled semiconductor lasers with time-delayed feedback are promising for the implementation of reservoir computing [23,24] with simple experimental apparatus. The evaluation of the complexity and dimensionality of coupled semiconductor lasers is quite important for this application, because it determines information capacity embedded in the dynamical systems. Our method for the evaluation of complexity and dimensionality is necessary for the application to reservoir computing.

VII. CONCLUSION

We have investigated consistency of response in unidirectionally coupled semiconductor lasers with optical feedback and measured the complexity of the coupled laser system by using Lyapunov spectrum analysis. We have found that the complexity of the entire laser system can be classified into three regions. When the response of the laser system shows consistency, the complexity of the entire (drive and response) laser system corresponds to that of the solitary drive laser. In the inconsistency region, the complexity of the entire laser system corresponds to the sum of the complexity of the solitary drive and response lasers. The complexity increases further near the boundary of the consistency region, where new dynamical fluctuations occur due to the nonlinear frequency mixing between the two optical-carrier components. We found that the complexity of the entire laser system strongly depends

on the degree of consistency. The results could be useful for the evaluation of complexity in coupled laser systems for the applications to physical one-way function and reservoir computing.

[1] Z. F. Mainen and T. J. Sejnowski, Science **268**, 1503 (1995).

[2] K. Klemm and S. Bornholdt, Proc. Natl. Acad. Sci. USA **102**, 18414 (2005).

[3] T. Pérez and A. Uchida, Phys. Rev. E **83**, 061915 (2011).

[4] A. Uchida, R. McAllister, and R. Roy, Phys. Rev. Lett. **93**, 244102 (2004).

[5] A. Uchida, K. Yoshimura, P. Davis, S. Yoshimori, and R. Roy, Phys. Rev. E **78**, 036203 (2008).

[6] A. Uchida, *Optical Communication with Chaotic Lasers, Applications of Nonlinear Dynamics and Synchronization* (Wiley-VCH, Weinheim, 2012).

[7] H. D. I. Abarbanel, N. F. Rulkov, and M. M. Sushchik, Phys. Rev. E **53**, 4528 (1996).

[8] A. S. Pikovsky, M. Rosenblum, and J. Kürths, *Synchronization* (Cambridge University Press, Cambridge, 2001).

[9] L. Moniz, T. Carroll, L. Pecora, and M. Todd, Phys. Rev. E **68**, 036215 (2003).

[10] T. Yamamoto, I. Oowada, H. Yip, A. Uchida, S. Yoshimori, K. Yoshimura, J. Muramatsu, S. Goto, and P. Davis, Opt. Express **15**, 3974 (2007).

[11] I. Oowada, H. Ariizumi, M. Li, S. Yoshimori, A. Uchida, K. Yoshimura, and P. Davis, Opt. Express **17**, 10025 (2009).

[12] R. Toral, C. R. Mirasso, E. Hernandez-Garcia, and O. Piro, Chaos **11**, 665 (2001).

[13] C. Zhou and J. Kürths, Phys. Rev. Lett. **88**, 230602 (2002).

[14] J. N. Teramae and D. Tanaka, Phys. Rev. Lett. **93**, 204103 (2004).

[15] J. N. Teramae and T. Fukai, Phys. Rev. Lett. **101**, 248105 (2008).

[16] H. Nakao, K. S. Arai, K. Nagai, Y. Tsubo, and Y. Kuramoto, Phys. Rev. E **72**, 026220 (2005).

[17] H. Nakao, K. Arai, and Y. Kawamura, Phys. Rev. Lett. **98**, 184101 (2007).

[18] K. Yoshimura, I. Valiusaityte, and P. Davis, Phys. Rev. E **75**, 026208 (2007).

[19] K. Yoshimura, J. Muramatsu, and P. Davis, Physica D **237**, 3146 (2008).

[20] C. S. Zhou, J. Kurths, E. Allaria, S. Boccaletti, R. Meucci, and F. T. Arecchi, Phys. Rev. E **67**, 066220 (2003).

[21] R. Pappu, B. Recht, J. Taylor, and N. Gershenfeld, Science **297**, 2026 (2002).

[22] K. Yoshimura, J. Muramatsu, P. Davis, T. Harayama, H. Okumura, S. Morikatsu, H. Aida, and A. Uchida, Phys. Rev. Lett. **108**, 070602 (2012).

[23] L. Appeltant, M. C. Soriano, G. Van der Sande, J. Danckaert, S. Massar, J. Dambre, B. Schrauwen, C. R. Mirasso, and I. Fischer, Nature Commun. **2**, 468 (2011).

[24] L. Larger, M. C. Soriano, D. Brunner, L. Appeltant, J. M. Gutierrez, L. Pesquera, C. R. Mirasso, and I. Fischer, Opt. Express **20**, 3241 (2012).

[25] R. López-Ruiz, H. L. Mancini, and X. Calbet, Phys. Lett. A **209**, 321 (1995).

[26] M. T. Martin, A. Plastino, and O. A. Rosso, Physica A **369**, 439 (2006).

[27] C. Bandt and B. Pompe, Phys. Rev. Lett. **88**, 174102 (2002).

[28] L. Zunino, M. C. Soriano, I. Fischer, O. A. Rosso, and C. R. Mirasso, Phys. Rev. E **82**, 046212 (2010).

[29] M. C. Soriano, L. Zunino, O. A. Rosso, I. Fischer, and C. R. Mirasso, IEEE J. Quantum Electron. **47**, 252 (2011).

[30] P. W. Lamberti, M. T. Martin, A. Plastino, and O. A. Rosso, Physica A **334**, 119 (2004).

[31] A. L. Franz, R. Roy, L. B. Shaw, and I. B. Schwartz, Phys. Rev. Lett. **99**, 053905 (2007).

[32] K. E. Chlouverakis, A. Argyris, A. Bogris, and D. Syvridis, Physica D **237**, 568 (2008).

[33] K. Pyragas, Phys. Rev. E **58**, 3067 (1998).

[34] R. Vicente, J. Dauden, P. Colet, and R. Toral, IEEE J. Quantum Electron. **41**, 541 (2005).

[35] R. Lang and K. Kobayashi, IEEE J. Quantum Electron. **16**, 3471 (1980).

[36] J. Ohtsubo, *Semiconductor Lasers, -Stability, Instability and Chaos*, 2nd ed. (Springer-Verlag, Berlin, 2008).

[37] H. Aida, M. Arahata, H. Okumura, H. Koizumi, A. Uchida, K. Yoshimura, J. Muramatsu, and P. Davis, Opt. Express **20**, 11813 (2012).

[38] N. Shibasaki, A. Uchida, S. Yoshimori, and P. Davis, IEEE J. Quantum Electron. **42**, 342 (2006).

[39] J. D. Farmer, Physica D **4**, 366 (1982).

[40] S. Wieczorek, T. B. Simpson, B. Krauskopf, and D. Lenstra, Phys. Rev. E **65**, 045207 (2002).

[41] S. Wieczorek, Phys. Rev. E **79**, 036209 (2009).

[42] S. Wieczorek and W. W. Chow, Opt. Commun. **282**, 2367 (2009).

[43] K. Kanno and A. Uchida, Nonlinear Theory and Its Applications, IEICE **3**, 143 (2012).

[44] A. Uchida, K. Amano, M. Inoue, K. Hirano, S. Naito, H. Someya, I. Oowada, T. Kurashige, M. Shiki, S. Yoshimori, K. Yoshimura, and P. Davis, Nature Photonics **2**, 728 (2008).

[45] M. Breakspear, J. R. Terry, and K. J. Friston, Neurocomputing **52**, 151 (2003).

[46] G. Giacomelli, S. Barland, M. Giudici, and A. Politi, Phys. Rev. Lett. **104**, 194101 (2010).